

Research Journal of Pharmaceutical, Biological and Chemical Sciences

Effect of Inorganic Filler in the Structural and Optical Properties of Polyether Sulfone

EM Abdelrazek¹, AM Abdelghany*², AH Oraby¹ and MA Morsi¹

¹Physics Dept., Faculty of Science, Mansoura Univ., Mansoura, 35516, Egypt.

²Spectroscopy Dept, Physics Division, National Research Center, Cairo, 12311, Egypt.

ABSTRACT

Casting technique was employed for preparation of polyether sulfon (PES) films with and without various mass fractions of inorganic filler (FeCl_3). Dependence of certain physical properties was correlated with filling level (FL). It is observed that upon increasing filler FeCl_3 concentrations, FTIR spectrum shows a formation of new band at 474 cm^{-1} which attributed to Fe-S stretching, and shift in other bands. These results manifested the conclusion about the specific interaction in polymer matrices and hence the occurrence of complexation. UV-Vis. data indicate the presence of a well defined π - π^* transition associated with the formation of conjugated electronic structure and the decrease in the optical energy gap was correlated to increase of the degree of disorder and overlap in the localized states. X-ray diffraction pattern (XRD) reveals the amorphous nature of the pristine and filled polymer and shows the random distribution of the filler within the polymeric matrix. Scanning electron micrograph (SEM) suggests the dependence of morphological structure on FL.

Keywords: FeCl_3 , PES, FTIR, UV-Visible, X-ray diffraction, DSC.

**Corresponding author*

INTRODUCTION

Polymeric materials have attracted considerable attention due to their stunning growth of interesting potential applications. Among such materials Polyether Sulfone (PES) which is a preferred material because it is a relatively new high temperature amorphous engineering thermoplastic with excellent thermal stability and oxidative stability [1]. Due to its optimum insulating properties, PES has applications in the electronics, automobiles industries, medical sector, food sector and aircraft cabins [2]. Polyethersulfone (PES) is finding extensive use in electronics due to its excellent dielectric property. In fact, PES is now rapidly becoming the material of choice for membrane preparation of hollow fibers [3, 4], stable substrate for the deposition and thermal processing of semiconductor thin films [5], sensors applications [6], etc. Moreover, PES is commercially available, relatively inexpensive and exhibits a high glass transition temperature ($T_g \sim 503$ K).

Recently transition metal ions have been extensively used as fillers in organic polymers because of the partially filled d-electron shells of very interesting properties [7–10] especially, physical properties [11]. Ferric chloride, FeCl_3 , with trivalent iron ions of $3d^5$ electron configurations was selected as filler due to its magnificent magnetic and electrical properties [7-10, 12, 13].

Moreover, FeCl_3 has been reported to give the most stable material, an aspect of importance when considering applications [10]. Most studies considered the FeCl_3 filler as an efficient electron acceptor and this was attributed to the formation of $\text{Fe}_2\text{Cl}_4^{-2}$ [14].

In previous works, our research group investigated the physical properties of PVDF films filled with different ratio of FeCl_3 [15] and also PEMA films filled with FeCl_3 [16].

The present work is mainly focused on the structural, Optical, electrical and magnetic properties of PES filled with transition metal chloride (FeCl_3) at different filling levels.

MATERIALS AND METHODS

Materials

Polyethersulfone (PES) granular was obtained from General Electric Company (Victrex 4100P), FeCl_3 pure reagent grade, (DEMISO, 99.5%) was used as a solvent for film preparation. All the chemical products were used without any further purification. The studied PES films filled with different ratio of ($x \text{ FeCl}_3$ wt%), $x = 0, 1, 2, 5, 10, 15$ were prepared by casting method. Dimethylsulfoxide (DEMISO) was used to dissolve the used materials. The solution of transition metal halide was added to the dissolved polymer at a suitable viscosity. The mixture was cast to a glass dish and kept in a dry atmosphere at 323 K for complete evaporation and removal of any solvent traces. The thickness of films was in the range of 0.10–0.20 mm.

Characterization techniques

X-ray diffraction (XRD) scans were obtained using PANalytical X'Pert PRO XRD system using Cu K α radiation (where, $\lambda = 1.540 \text{ \AA}$, the tube operated at 30 kV, the Bragg's angle (2θ) in the range of 5-80°). Fourier Transform Infrared (FTIR) measurements were carried out using single beam Fourier transform-infrared spectrometer (Nicolet iS10, USA) at room temperature in the spectral range from 4000-400 cm $^{-1}$. UV/Vis. absorption spectra were measured in the wavelength region of 222-800nm using spectrophotometer (V-570 UV/VIS/NIR, JASCO, Japan). Morphology and surface characteristics were studied using scanning electron microscope using (JEOL 5300, Tokyo, Japan), operating at 30 kV accelerating voltage. Surface of the samples were coated with a thin layer of gold (3.5 nm) by the vacuum evaporation technique to minimize sample charging effects due to the electron beam.

RESULTS AND DISCUSSION

Fourier transform infrared analysis

Fourier transform infrared (FTIR) spectroscopy was employed to identify the different structure groups in the polymer matrices and to retrace the structural changes result from introducing filling material. Fig.1 shows FTIR absorption spectra of virgin PES and samples that filled with various levels of FeCl $_3$ at room temperature in the region 4000–400 cm $^{-1}$. The spectra of all samples are quite similar and a little obvious change was recognized. FTIR absorption bands positions and the assignments of all prepared samples are listed in Table 1.

From these spectrum a broad band at 3309–3600 cm $^{-1}$ that is associated with the OH stretching of water molecules since there is no OH band in the pristine PES structure. Presence of FeCl $_3$ may lead to further increase in the water content in the prepared samples [17]. Also, the method of preparation (casting method) may indeed result in the presence of entrapped water [18].

This behavior was also observed by Belfer and colleagues for the millipore PES membrane [19]. Many authors [15, 16, 20] also observe the same behavior of films prepared by casting method. The water molecules were difficult to be removed completely [19], despite the fact that all the prepared samples were kept in an oven for 4 days at 70 °C.

C-H symmetrical stretching vibration occurs in the range 3139 - 3033 cm $^{-1}$ which decreases with increasing filler concentration. The band at about 2603 cm $^{-1}$ is assigned to weak S-H stretching [21] which shifts to lower wave numbers at high concentrations of FeCl $_3$. In the 2000 –1670 cm $^{-1}$ region, a series of weak combination and overtone bands appears and the pattern of the overtone bands reflects the substitution pattern of the benzene ring [21, 22].

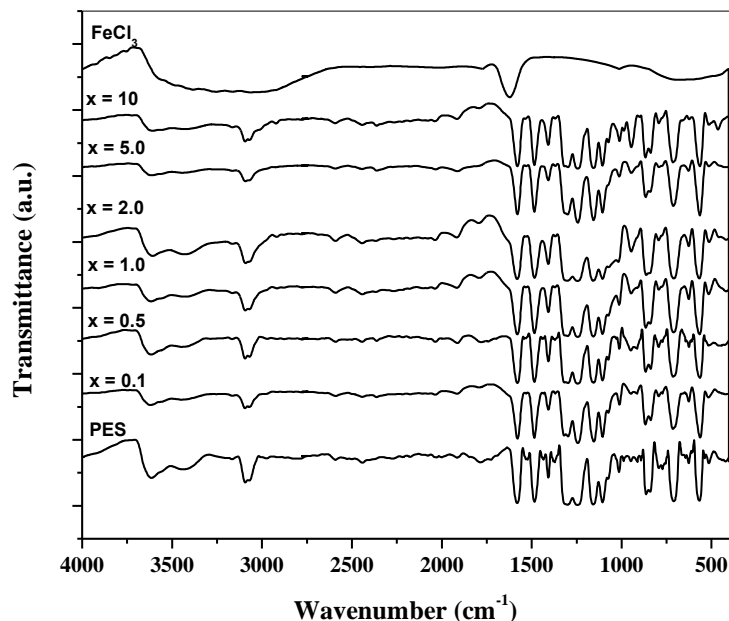


Fig.1. Infrared spectra of PES films filled with various mass fractions of FeCl_3

Skeletal vibrations, representing C=C stretching vibration of benzene ring occurs in the region $1652\text{--}1457\text{ cm}^{-1}$ indicates the formation of small conjugated polyene sequences, which are presumably responsible for the color of the fillers-treated PES, the changes which appear in this band for different FLs point to the possibility of Fe to be attached to a C=C group in the side chain of the PES molecule. This band can be considered as suitable sites for polarons and/or bipolarons to be in the polymeric matrix [23-26].

The asymmetric stretch (ν_{asym}) of the aromatic ether group (Ar-O-Ar) appears at 1255 cm^{-1} . The bands due to the asymmetric (1321 cm^{-1}) and symmetric (1164 cm^{-1}) stretches of the sulfone group, O=S=O, are clearly identified [27, 28].

The last three peaks reveal a maximum values at at $x=5.0$, $x=0.1$ and minimum values at $x=2.0$. The absorption band due to the symmetric stretching of C-O-C and aryl sulfone appears in the region $1097\text{--}1457\text{ cm}^{-1}$ [29].

The band at 1108 cm^{-1} refers to S=O stretching [21, 31]. It is remarkable that the present double bond segments are considered as suitable sites for polarons and/or bipolarons [30].

C-H in the plane deformation vibration appears at $1018, 991\text{ cm}^{-1}$ while Out-of-plane C-H bending appears at 919 cm^{-1} [21]. The intensity of the bands also decreases with increasing the FLs of filler. In the pristine PES, SO_2 scissoring is observed at 576 cm^{-1} [27,28]. The intensity of this band decreases largely specially at high FLs of filler, specially, ($x=10.0$).

Table (1) FTIR band position and their assignments for the prepared samples

Band position (cm ⁻¹)	Band assignment	Ref.
3309-3600	Broad intermolecular hydrogen bonded,-OH stretching	15-20
3139-3033	Aromatic C-H stretching	21
2453	Moderately weak S-H stretching	21
2000-1670	Overtone-combination bands	21, 22
1588, 1490, 1400	The C=C ring stretching	23-26
1321	Sulfone group ,O=S=O asymmetric stretching	27,28
1255	Aromatic ether (Ar-O-Ar) asymmetric stretching	27,28, 29
1164	Sulfone group ,O=S=O symmetric stretching	27,28
1108	S=O stretching	21, 31
1081	C-O-C stretching	29
1016, 991	In-plane C-H bending	21
950, 870	O=S-Fe stretching	31, 34
919, 894	Out- of- plane C-H bending	21
846	C-C stretching	21
796	C-Cl stretching	21
574	SO ₂ Scissoring	27, 28
520	Weak S-S stretching	21
474	Fe-S stretching	21

It is also seen that the characteristic bands due to PES substrates are retained in the case of samples of filled PES/FeCl₃. There is indication of new bands appearing at 954 and 867 cm⁻¹, located at wavenumbers slightly lower than those corresponding to the S=O stretch in PES. In previous studies on DMSO complexes with different metals, it has been found that the S=O stretch at 1100-1055 cm⁻¹ is lowered to 960-930 cm⁻¹ when the coordination of the metal occurs through the oxygen of DMSO: when the coordination of the metal occurs through sulfur, the S=O stretch shifts to higher wave numbers, 1157-1116 cm⁻¹ [31]. The new absorption bands may be correlated likewise to defects induced by the charge-transfer reaction between the polymer chain and the dopant [32-34].

The absorption band at about 954 cm⁻¹ was found to be characteristic of the syndiotactic structure of the prepared films.

The observed peak at 798 cm⁻¹ is assigned to C-Cl stretching and C-H bending, exhibits changes in its intensity behavior with FeCl₃ concentrations. The apparently change in the intensity of this peak with FeCl₃ means that this peak is sensitive to some type of defects, which may be head-to-head [(h-to-h)] and tail to- tail [(t-to-t)] polymer chain defects [35, 36]. The h-to-h defects are found to be suitable site for polarons and/or bipolarons in the PES matrix [37].

The absorption band at 846 [21] cm⁻¹ is attributed to C-C stretching. Out-of-plane aromatic C-H bend appears at (monosubstituted benzene ring) 919, 894 cm⁻¹. Low-frequency bands are of little use in determining the nature of ring substitution since these absorption patterns result from the interaction of O=S=O and C-H out-of-plane frequencies. The absorption region 547-497 cm⁻¹ corresponds to weak S-S stretching [21] and the new band at 474 cm⁻¹ can be attributed to Fe-S stretching which confirms the complexation between filler and polymer.

From the IR spectra, it is observed that upon increasing the filler FeCl_3 concentrations, some of the peaks are shifted, new bands appeared and some of them disappear with respect to the pure PES. These results manifested the conclusion about the specific interaction in polymer matrices and hence the occurrence of complexation [38].

Ultraviolet and visible analysis

Ultraviolet–visible (UV–Vis.) spectroscopy is an important tool for investigation as it gives an idea about the value of optical band gap energy (E_g). The absorption of light energy by polymeric materials in UV and visible regions involves promotion of electrons in σ , π , and η orbital from the ground state to higher energy states which are described by molecular orbitals [39].

The results of absorption studies with UV–Vis. spectrophotometer in the wavelength range of 200–900 nm carried out on virgin and filled samples are illustrated in Fig. 2. The optical absorption spectrum of the virgin sample shows an absorption edge which has a sharp decrease with increasing wavelength upto ~ 314 nm, followed by plateau region. The observed spectra are characterized by the main absorption edge for all curves that shifted towards higher wavelength with increase the filler content. These shifts indicate the complexation the miscibility between the filler and the polymer, and may also be due to change in crystallinity due to adding the filler [40]. It is evident that optical absorption increases with increasing fluence and this absorption shifts from UV–Vis towards the visible region for irradiated samples. The increase in absorption may be attributed to the formation of a conjugated system of bonds due to bond cleavage and reconstruction [41].

The absorption band (shoulder) of pure PES at about 274 nm may be attributed π - π^* which comes from unsaturated bonds, mainly (C=O and/or C=C /or S=O) [42-44].

The sharp absorption edge around 245 nm in pure PES is due to the semicrystalline nature of PES. PES contains single bonds in the main chain and double bonds in the branches; the noted absorption in the UV (200–300 nm) region is interpreted [45].

The bands in the range of 370–500nm are due to crystal field transitions of the tetrahedral isolated Fe^{+3} ions [46]. Some of the observed band positions and their assignments are given in Table 2. The FL dependence of the intensity of the band at 364 nm is shown in Fig. 3. This reveals that content of tetrahedral Fe^{+3} in the hosted polymer increases as concentration of filler FeCl_3 increases and the presence of Fe-ion in the filled samples.

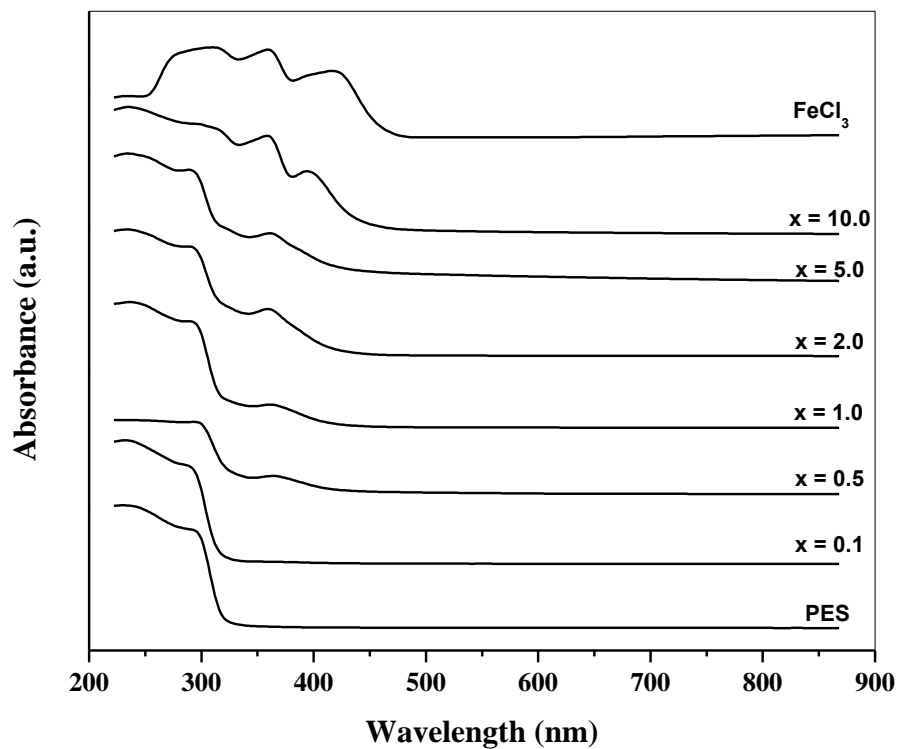


Fig.2. UV-Vis. spectra of pure and PES filled with different concentrations of FeCl_3 .

Table 2; Observed band positions and their assignments for the tetrahedral Fe^{+3}

FeCl_3 (wt%)	Observed Wavelength (nm)	Transitions ${}^6\text{A}_{1g}(\text{S}) \rightarrow$
0.1	294	${}^4\text{T}_{1g}(\text{P})$
	366	${}^4\text{T}_{2g}(\text{D})$
0.5	302	${}^4\text{T}_{1g}(\text{P})$
	370	${}^4\text{T}_{2g}(\text{D})$
1.0	296	${}^4\text{T}_{1g}(\text{P})$
	368	${}^4\text{T}_{2g}(\text{D})$
2.0	298	${}^4\text{T}_{1g}(\text{P})$
	364	${}^4\text{T}_{2g}(\text{D})$
5.0	296	${}^4\text{T}_{1g}(\text{P})$
	368	${}^4\text{T}_{2g}(\text{D})$
10	304	${}^4\text{T}_{2g}(\text{D})$
	364	${}^4\text{T}_{2g}(\text{D})$
	406	${}^4\text{E}_g(\text{G})$

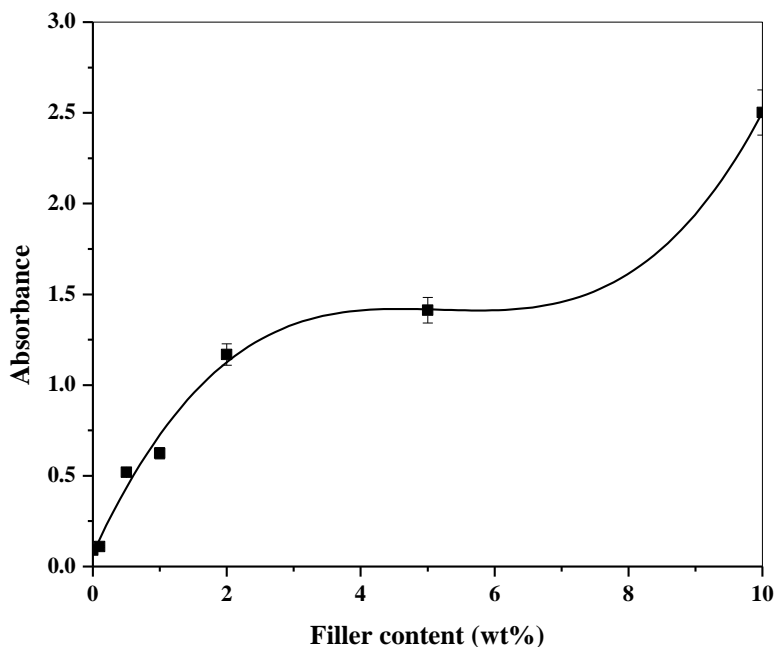


Fig.3. FL dependence of absorption peaks at 364 nm.

Determination of optical energy gap (E_g)

The optical absorption method can be used for the investigation of the optically induced transitions and can provide information about the bond structure and energy gap in crystalline and non-crystalline materials [47].

The study of optical absorption gives information about the band structure of organic compound. Semiconductors are generally classified into two types: (i) direct band gap and (ii) indirect band gap. In direct band gap, the top of the valence band and the bottom of conduction band both lay at the same zero crystal momentum (wave vector). If the bottom of conduction band does not correspond to zero crystal momentum, then it is called indirect band gap. In indirect band gap materials transition from valence to conduction band should always be associated with a phonon of the right magnitude of crystal momentum [48]. Davis and Shalliday [49] reported that near the fundamental band edge, both direct and indirect transitions occur and can be observed by plotting $(\alpha h\nu)^{1/2}$ as a function of photon energy ($h\nu$). The analysis of Thutupalli and Tomlin [50] is based on the following relations:

$$(n\alpha h\nu)^2 = c_1 (h\nu - E_{gd}) \quad (1)$$

$$(n\alpha h\nu)^{1/2} = c_2 (h\nu - E_{gi}) \quad (2)$$

Where $h\nu$ is the photon energy, E_{gd} , the direct band gap, E_{gi} , the indirect band gap, n , integer, c_1 , c_2 , constants and α is the absorption coefficient.

The absorption coefficient (α) can be determined as a function of frequency using the formula [51]:

$$\alpha = 2.303 \times (A / d) \quad (3)$$

Where **A** is the absorbance and **d** is the thickness of the sample under investigation. By plotting $(\alpha h\nu)^{1/2}$ versus photon energy ($h\nu$), each linear portion indicates a band energy gap (E_g). It is will be noticed that the curves are characterized by the presence of an exponentially decay tail at low energy [52].

From the linear parts of these curves, the E_g values of the films were calculated and are given in Table 3. The absorption edge shifts the higher wavelengths with increasing FeCl_3 content. This suggests that the optical band gap decreases with FeCl_3 content as shown in Fig.5. It is clear that E_g decreases as W increases. This indicates that the FeCl_3 filler significantly influence optical energy gap.

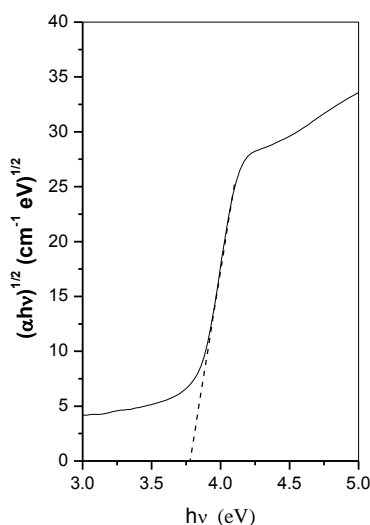
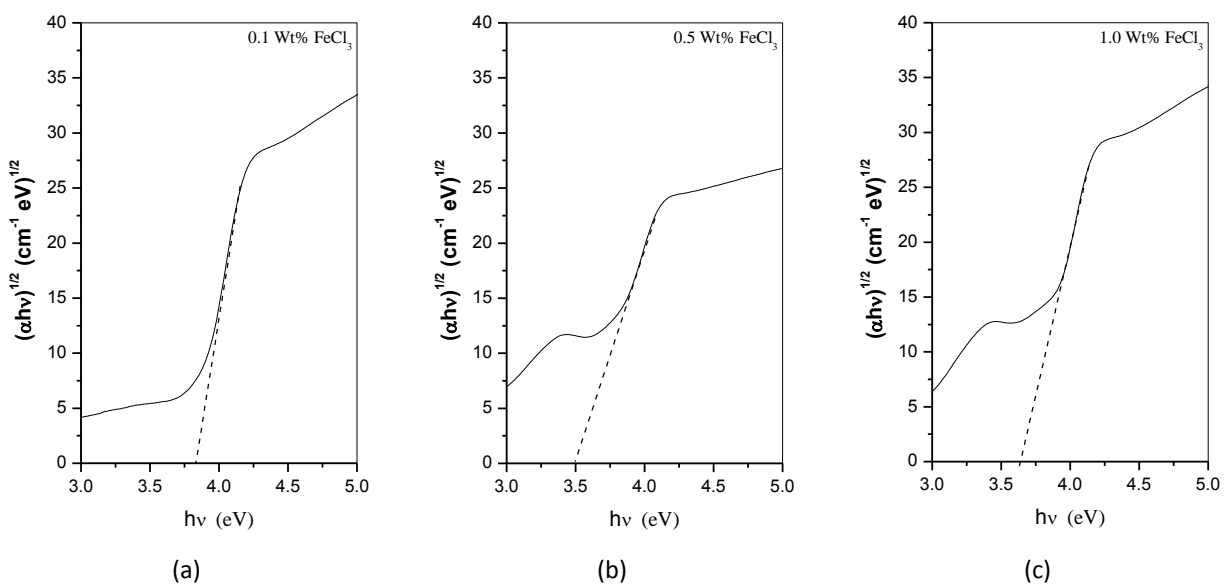


Fig. (4.a) Relation between photon energy ($h\nu$) versus $(\alpha h\nu)^{1/2}$ for pristine polymer.



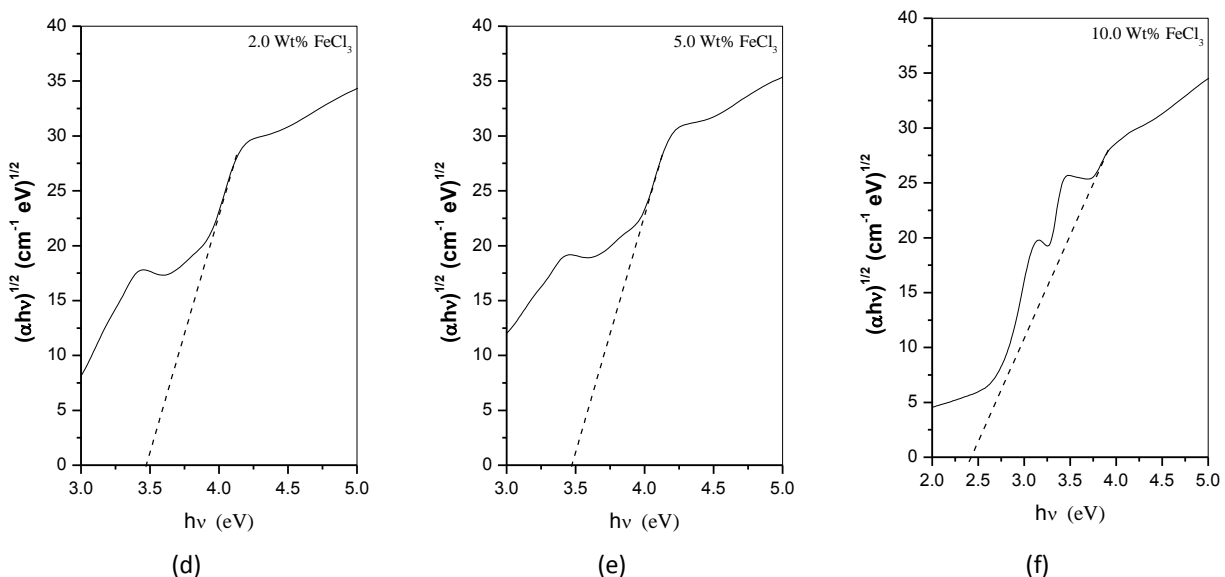


Fig. (4.b-d) Relation between photon energy ($h\nu$) versus $(\alpha h\nu)^{1/2}$ for filled polymer.

Table 3: Absorption edge (λ_g) and optical energy gap (E_g) for prepared samples.

FeCl ₃ (wt%)	Absorption edge (λ_g) (nm)	E_g (eV)
0.00	330.80 ± 13.8	3.67
0.10	342.14 ± 15.5	3.63
0.50	416.78 ± 19.6	2.98
1.00	450.0 ± 23.9	2.67
2.00	470.45 ± 25.9	2.64
5.00	494.82 ± 28.2	2.51
10.0	513.22 ± 30.4	2.42

The addition of FeCl₃ content into polymer creates a consequent effect on the optical band gap. FeCl₃ content is responsible for the formation of some defects in the films. These defects produce the localized states in the optical band gap. The density of the localized states is found to be proportional to the concentration of the defects [53]. The FeCl₃ dopant may cause the changes in the localized states to overlap.

These overlaps give an evidence for decreasing energy band gap when FeCl₃ content is increased in the polymeric matrix [54, 55]. The decrease in the optical band gap can be explained by the increase in the degree of disorder in the films. The presence of the high content causes expanding of the localized energy levels. Therefore, the decrease in the optical band gap results from the localized states having high content. These results indicate the presence of a well defined π - π^* transition associated with the formation of conjugated electronic structure [56].

The optical band gap dependence of FeCl₃ content is shown in Fig. 5.

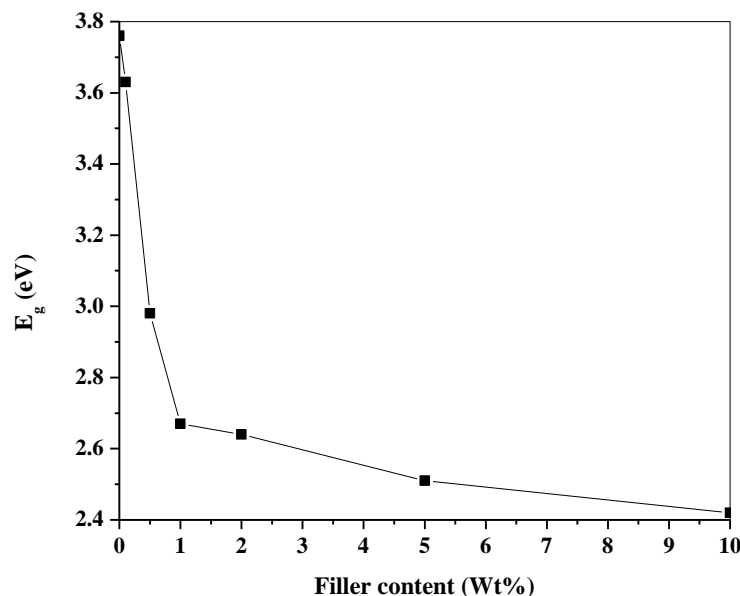


Fig. 5. Variation of the optical band gap of thin films with FeCl_3 content

The shift in absorption edge was correlated with the optical band gap E_g , as Table .3, given by;

$$E_g = hc / \lambda_g \quad (4)$$

Where h is Planck constant and c is the velocity of light. The wavelength λ_g is determined by Tauc's expression [57] from the intersection with the abscissa of the plot of $(\epsilon^{1/2}/\lambda)$ versus $(1/\lambda)$ where ϵ is the optical absorbance and λ is the wavelength. The absorption edge moves towards higher wavelengths.

X-ray diffraction analysis

The polymer studied here is a complex polymer widely used in electronics and sensors applications falling in the category of polymeric materials that consist of crystalline and amorphous regions in different proportions. XRD measurements have been carried out for pristine samples and samples with various filling levels of FeCl_3 to observe changes in structure crystallinity.

It is worth quoting that no evidence of X-ray crystallinity was found in any of the tested PES samples or samples that doped with different filling level of FeCl_3 . Blackadder and Ghavamikia [58] concluded that PES is undoubtedly crystalline on the evidence of outward appearances. The main aim of the measurement is to check crystallization of PES films with and without filler. It must be pointed out that crystallinity of polymers is one of the factors determining their transport properties [59].

Fig.6. shows the XRD pattern for virgin and filled PES films with FeCl_3 with various mass fractions (x) namely ($x = 0.0, 0.1, 0.5, 1.0, 2.0, 5.0,$ and 10.0%).

The diffraction pattern of virgin PES indicates that this polymer is mainly amorphous in nature and shows one prominent X-ray peak at $2\theta = 17.91^\circ$.

A comparison in terms of peak position, peak intensity, FWHM and relative area A_T have been carried out and summarized in table 4.

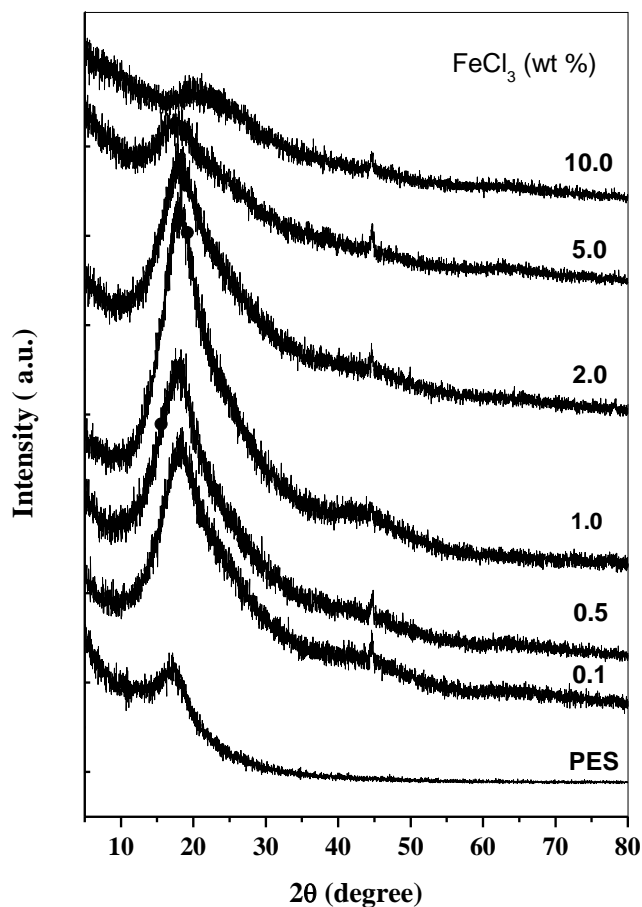


Fig. 6 The X-ray diffraction scans for variously filled PES with $FeCl_3$

Table.4 peak position, peak intensity, FWHM and relative area A_T of filled PES samples with $FeCl_3$

$FeCl_3$ (wt %)	Peak Position (2θ)	Peak Intensity	F.W.H.M (2θ)	Relative Area (cm^2)
0.00	17.91	292	4.64	2.30
0.10	18.99	671	5.76	9.25
0.20	18.77	728	5.62	9.46
0.50	18.95	917	4.60	13.53
1.00	18.99	635	5.80	9.76
5.00	18.35	431	7.03	4.52
10.0	21.49	304	9.48	0.37

The present X-ray scans revealed a very significant change in the halo position due to the $FeCl_3$ filling. These apparent changes in band position, especially at high conc. of $FeCl_3$ point

out that the FeCl_3 used in this study seemed to alter weakly the average intersegmental spacing of polymer chains (i.e. this implies that the lattice parameters do not change significantly). On the other hand, the PES films containing FeCl_3 spectrum showed a sharp peak at $2\theta = 19^\circ$. This result indicates that the addition of FeCl_3 at ($x = 0.5$ wt%) can cause structural variations in the polymeric network [60]. The position of the sharp peak coincided with a peak at $2\theta = 19^\circ$ in the X-ray scans of pure FeCl_3 , as shown in Fig. 6. This confirms the presence of FeCl_3 crystallites within the polymeric matrix [61]. But, at 1.0 % FL, this peak is represented by a low intensity and broad shape. It might have arisen from scattering atomic planes of some crystalline patterns of the PES- Fe^{+2} complex. This slight disappearance of the shape of the second peak may be attributed to the change of the mode of chelation of the FeCl_3 filler.

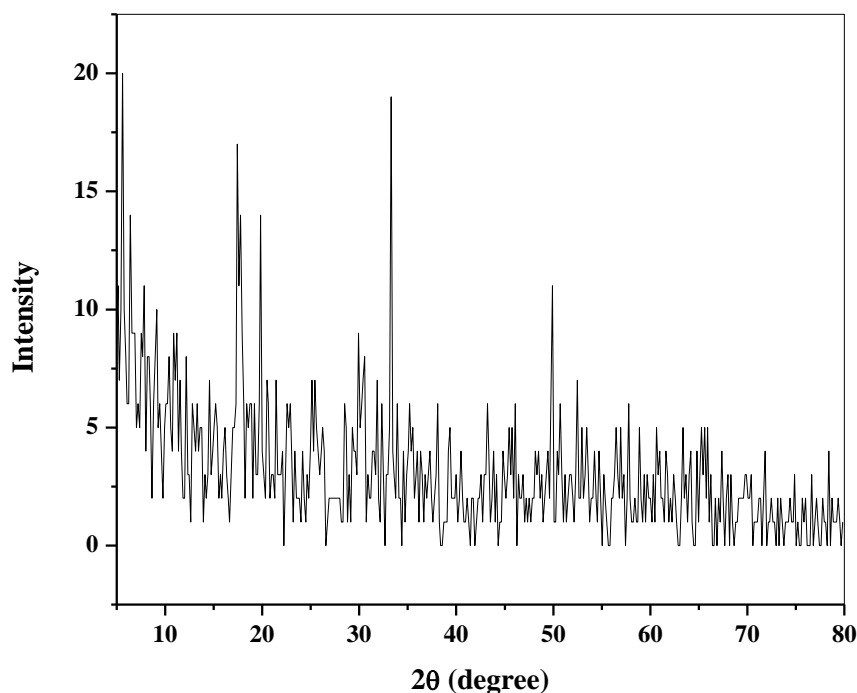


Fig.7. X-ray scans of pure FeCl_3

The area under the amorphous peak centered at $2\theta = 17.91^\circ$. (A_T) can be taken as a measure for the degree of crystallinity. It is clear that A_T increases as W increases, until FL 1.0 % and then decreases indicating that the fillers significantly influence the degree of crystallinity [62].

At 1% FL, the intensity of diffraction peak has a maximum value implying the more organized distribution of the FeCl_3 filler in the polymeric matrix. With increasing the content of FeCl_3 and at 2% FL, there is a dramatic decrease in the intensity of the diffraction peak. At 5.0, 10.0% FL, the amorphous peaks became broad and a significant decrease in its intensity was observed indicating that the distribution of the FeCl_3 filler in the polymeric matrix became random.

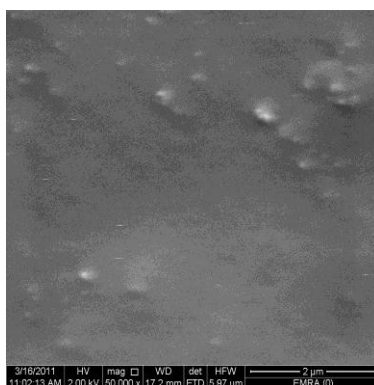
Scanning Electron Microscopy (SEM)

Morphology of the studied samples was investigated with SEM to provide further information about the structural modifications of PES films due to filling with FeCl_3 . Scanning electron micrograph (SEM) suggests the dependence of morphological structure on FL. Figure (8) shows the SEM micrograph of the surface of pure and filled films with different concentrations of FeCl_3 at magnification 50,000times. Figure (8-a) shows pure polymer morphology which is transparent and is shown to be in a uniform morphology revealing a rather smooth surface. Figure (8-b) shows some pores between the PES and FeCl_3 interface could be observed, which became large pores of different size and pores groups randomly distribution in a medium as shown in figure (8-c). This can be attributed to the partial compatibility between the polymer and the filler.

By increasing the concentration of the additives to 1 wt%, a large granules and granule groups randomly distribution in a medium that appeared to be pure PES as shown in figure (8-d). The grown ones were of different sizes and irregular shapes, uniformly distributed in the amorphous matrix, indicating the occurrence of a homogeneous growth mechanism, which is also observed in figure (8-e).

On the other hand, the micrograph of $x = 5.0\%$ as shown in figure (8-f) is characterized by the presence of two types of granules: unseparated and separated ones of deformed shapes.

An interesting pattern is observed for the case of $x=10.0\%$ which contains a highly condensed number of very small granules. This pattern can be correlated with findings the optical absorption, in which a maximum content of tetrahedral Fe^{3+} is found at $x = 10.0\%$. Therefore, the high concentration of tetrahedral Fe^{3+} may be considered as the main reason for the pattern of Figure. (8-g).



(a)

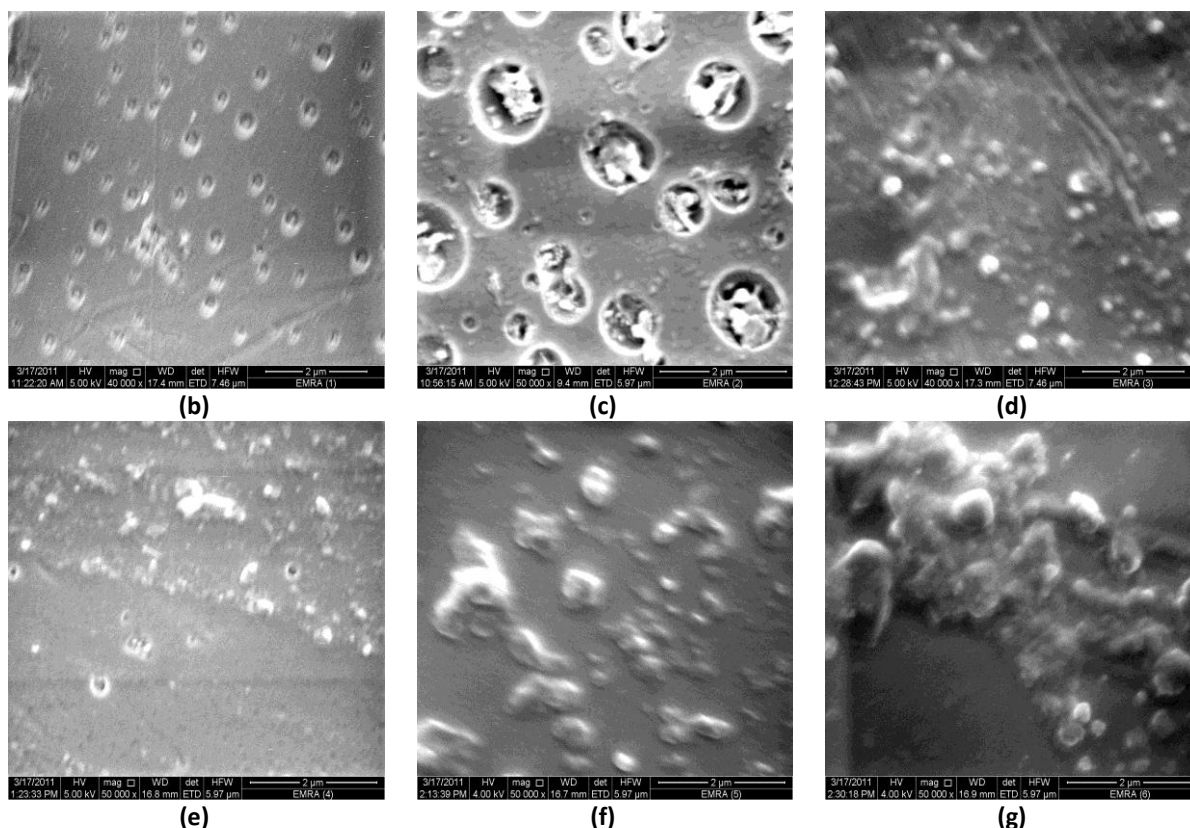


Fig.(8.a-g) Scanning electron micrograph with and without doping.

These results showed the formation of a crystalline phase, when PES was filled with FeCl_3 , that increased with an increasing W value of FeCl_3 . These results confirmed the findings of XRD in this work. This indicates segregation of the filler in the host matrix and this may be confirmed by the interaction and complexation between filler and polymer.

CONCLUSION

Casting technique was employed for preparation of pristine and filled polyether sulfon (PES) films with various mass fractions of inorganic filler (FeCl_3). Dependence of certain physical properties was correlated with filling level (FL). FTIR spectrum shows a formation of new band at 474 cm^{-1} which attributed to Fe-S stretching that confirms the complexation between filler and polymer. It is also observed that upon increasing the filler FeCl_3 concentrations, some of the peaks are shifted, new bands appeared and some of them disappear with respect to the pure PES. These results manifested the conclusion about the specific interaction in polymer matrices and hence the occurrence of complexation. UV-Vis. absorption spectra shows an absorption edge around 245 nm in pure PES which attributed to the semicrystalline nature of PES while the bands in the range of 370–500nm are due to crystal field transitions of the tetrahedral isolated Fe^{+3} ions. The content of tetrahedral Fe^{+3} in the hosted polymer increases as concentration of filler FeCl_3 increases and also the presence of Fe-ion in the filled samples. The decrease in optical energy gap was attributed to the increase of degree of disorder and to

the overlap in the localized states which also observed from XRD data. These results indicate the presence of a well defined π - π^* transition associated with the formation of conjugated electronic structure. X-ray scans revealed a very significant change in the halo position due to the FeCl_3 filling. It was observed that the fillers significantly influence the degree of crystallinity.

SEM results shows the formation of a crystalline phase which increases with increasing filler content, indicates segregation of the filler in the host matrix, these results confirm the findings of XRD and optical measurements.

REFERENCES

- [1] CHA Harper, EM Petrie, *Plastics Materials and Processes. A Concise Encyclopedia* 2003, 974 John Wiley & Sons, Inc., Hoboken, New Jersey, pp. 427.
- [2] <http://www.hostec.com/index.php?option=comcontent&task=view&id=10&Itemid=18>.
- [3] KC Khulbe, C Feng, T Matsuura, GC Kapantaidakis, M Wessling, GH Koops. *J Membr Sci* 2003; 226: 63-73.
- [4] Q Yang, TS Chung and YW Santoso. *J Membr Sci* 2007; 290: 153-163.
- [5] PK Nair, J Cardoso, O Gomez Daza and MTS. Nair. *Thin Solid Films* 2001; 401: 243-250.
- [6] G Gerlach, K Baumann, R Buchhold and A Naklal. German Patent D E 19853732, 1998.
- [7] AK Sharma, DS Sagar. *J Polym Int* 1990; 25(1): 43.
- [8] AK Sharma, V Adinarayana, DS Sagar. *J Polym Int* 1991; 25(3): 167.
- [9] A Tawansi, HI Abdelkader, W Balachandran, EM Abdelrazek. *J Mater Sci* 1994; 29: 4001.
- [10] P Kuivalainen, H Stubb, H Isotlo. *Phys Rev B* 1985; 32: 7900.
- [11] S Elhefnawy. Study of physical properties of some polymeric sensors for electromagnetic waves and its applications. Thesis, Mansoura University 1995.
- [12] A Tawansi, N Kinawy, M El-Mitwally. *J Mater Sci* 1989; 24: 2497.
- [13] A Tawansi, A El-Khodary, AE Youssef. *Int J Polym Mater* 54, in press.
- [14] P Kuivalainen. *Phys Rev B* 1985; 31(12): 7900.
- [15] A Tawansi, HI Abdelkader, EM Abdelrazek. *J Mater Sci Tech* 1997; 13: 194.
- [16] EM Abdelrazek. *Physica B* 2007; 400: 26.
- [17] GS Kapur, AS Brar. *J Radioanal Nucl Chem Letters* 1990; 2: 135.
- [18] A Rahimpour, SS Madaeni, AH Taheri, Y Mansourpanah. *J Membr Sci* 2008; 313: 158.
- [19] S Belfer, R Fainchtain, Y Purinson, O Kedem. *J Membr Sci* 2000; 172: 113.
- [20] W Zhao, et al. *J Membr Sci* 2010. doi:10.1016/j.memsci.2010.11.065.
- [21] B Stuart. *Modern Infrared Spectroscopy, ACOL Series*, Wiley, Chichester, UK, 1996.
- [22] G Socorates. *Infrared Characteristics: Group Frequencies*, Wiley, New York, 1980.
- [23] A Tawansi, AH Oraby, HI Abdelkader, M Abdelaziz. *J Magnetism and Magnetic Materials* 2003; 262: 203–211.
- [24] A Tawansi, HM Zidan, AH Oraby, ME Dorgham. *J Phys D Appl Phys* 1998; 31: 3428.
- [25] A Tawansi, HM Zidan, YM Moustafa, AH Eldumiaty. *Phys Scr* 1997; 55: 243.
- [26] A Tawansi, AH Oraby, HM Zidan, ME Dorgham. *Physica B* 1998; 254: 126.
- [27] N Colthup, L Daly, S Wiberley, *Introduction to Infrared and Raman Spectroscopy*, 2d ed. Academic press, New York, 1975.
- [28] C Pouchert, "The Aldrich Library of FT-IR Spectra", Aldrich Chemical, Milwaukee, 1985.

- [29] R Kumar et al. Nucl Instr Meth Phys Res 2006; 248B: 279–283.
- [30] A Tawansi, HI Abdelkader, M Elzalabany, EM Abdelrazek. J Mater Sci 1994; 29: 3451.
- [31] K Nakamoto. Infrared and Raman Spectra of Inorganic Compounds, Wiley-Interscience, Newyork, USA, 1978, pp. 344-345.
- [32] S Rajendran, M Sivakumar, R Subadevi. Mater Lett 2004; 58: 641.
- [33] M Nagura, S Matsu Zawa, K Yamamura, H Ishikawa. Polym J 1982; 14: 69.
- [34] PK Nair, J Cardoso, O Gomez Daza, MTS Nair. Thin Solid Films 2001; 407: 243-250.
- [35] M Kobayashi, K Tashiro, H Tadokoro. Macromolecules 1975; 8: 158.
- [36] M Silvakumar, R Subadevi, S Rajendran, NL Wu, JY Lee. Mater Chem Phys 2006; 97: 330.
- [37] A Tawansi, AH Oraby, EM Abdelrazek, M Abdelaziz. Polym Testing 1999; 18: 569.
- [38] A Tawansi, AH Oraby, EM Abdelrazek, MI Ayad, M Abdelaziz. J Appl Polym Sci 1998; 70: 1437.
- [39] JR Dyer. Application of Absorption Spectroscopy of Organic Compounds, Prentice-Hall, New Jersey, 1994.
- [40] EM Abdelrazek, IS Elashmawi. Polym Comp 2008; 29: 1036.
- [41] LS Farenza, RM Papaleo, A Hallen, MA Araujo, RP Livi, BUR Sundqvist. Nucl Instr Meth 1995; B105: 134.
- [42] EA Davis, NF Mott. Philos Mag 1970; 22: 403.
- [43] EM Abdelrazek, IS Elashmawi, A El-khodary, A Yassin. Current Applied Physics 2010; 10: 607–613
- [44] EM Abdelrazek. Physica 2008; B403: 2137.
- [45] KAM El-Kader, SF Abdel Hamied. J Appl Polym Sci 2002; 86: 1219.
- [46] B Hannover, M Lenlet, R Corles. J Non-Cryst Solids 1992; 151: 209.
- [47] AM Abdelghany, HA ElBatal, L Mari. Radiation Effects and Defects in Solids 2012; 167(1): 49-58.
- [48] CVS Reddy, AK Sharma, VVRN Rao. Polymer 2006; 47: 1318.
- [49] DS Davis, TS Shalliday. Phys Rev 1960; 118: 1020.
- [50] GM Thutupalli, SG Tomlin. J Phys D: Appl Phys 1976; 9: 1639.
- [51] IS Elashmawi, NA Hakeem. Polym Eng Sci 2008; 895: 48.
- [52] J Bardeen. Phys Rev 1949; 75: 169.
- [53] NF Mott. Philos Mag 1970; 24: 1.
- [54] HM Zidan, M Abu-Elnader. Physica 2005; B355: 308.
- [55] R Murri, L Schiavulli, N Pinto, T Ligonto. J Non-Cryst Solids 1992; 139: 60.
- [56] WR Salaneck, CR Wu, JL Bredas, JJ Ritsko. Chem Phys Lett 1986; 127: 88.
- [57] J Tauc, R Grigorovici, A Vaneu. Phys Status Solidi 1996; 15: 627.
- [58] DA Blackadder and H Ghavamikia. Polymer 1979; 20: 1433-1434.
- [59] G Chowdhury, B Kruczek and T Matsuura. Polyphenylene Oxide and Modified Polyphenylene Oxide Membranes: Gas, Vapour and Liquid Separation. Kluwer Academic Publishers, Dordrecht, The Netherlands, 2001.
- [60] HM Zidan. J Polym Sci: Part B: Polym Phys 2003; 41: 112.
- [61] A Tawansi, A EL-Khodary, HM Zidan, SI Badr. Polym Test 2002; 21: 381.
- [62] M Abdelaziz, EM Abdelrazek. Physica B 2004; 349: 84.